HAL
open science

Large-Scale Collective Properties of Self-Propelled Rods

Francesco Ginelli, Fernando Peruani, Markus Baer, Hugues Chaté

To cite this version:

Francesco Ginelli, Fernando Peruani, Markus Baer, Hugues Chaté. Large-Scale Collective Properties of Self-Propelled Rods. Physical Review Letters, 2010, 104 (18), pp.184502. 10.1103/PhysRevLett.104.184502 . hal-00905223

HAL Id: hal-00905223

https://hal.science/hal-00905223

Submitted on 18 Nov 2013

HAL is a multi-disciplinary open access archive for the deposit and dissemination of scientific research documents, whether they are published or not. The documents may come from teaching and research institutions in France or abroad, or from public or private research centers.

L'archive ouverte pluridisciplinaire **HAL**, est destinée au dépôt et à la diffusion de documents scientifiques de niveau recherche, publiés ou non, émanant des établissements d'enseignement et de recherche français ou étrangers, des laboratoires publics ou privés.

arXiv:0911.1924v1 [cond-mat.soft] 10 Nov 2009

Large-scale collective properties of self-propelled rods

Francesco Ginelli,[1,2] Fernando Peruani,[1] Markus Bär,[3] and Hugues Chaté[1]

[1] *Service de Physique de l'État Condensé, CEA–Saclay, 91191 Gif-sur-Yvette, France*
[2] *Institut des Systèmes Complexes de Paris Île-de-France, 57-59 rue Lhomond, 75005 Paris, France*
[3] *Physikalisch-Technische Bundesanstalt, Abbestrasse 2-12, 10587 Berlin, Germany*

(Dated: November 10, 2009)

We study, in two space dimensions, the large-scale properties of collections of constant-speed polar point particles interacting locally by nematic alignment in the presence of noise. This minimal approach to self-propelled rods allows one to deal with large numbers of particles, revealing a phenomenology previously unseen in more complicated models, and moreover distinctively different from both that of the purely polar case (e.g. the Vicsek model) and of active nematics.

PACS numbers: 05.65.+b, 87.18.Hf, 87.18.Gh

Collective motion is an ubiquitous phenomenon observable at all scales, in natural systems [1] as well as human societies [2]. The mechanisms at its origin can be remarkably varied. For instance, they may involve the hydrodynamic interactions mediated by the fluid in which bacteria swim [3], the long-range chemical signaling driving the formation and organization of aggregation centers of Dictyostelium discoideum amoeba cells [4], or the local cannibalistic interactions between marching locusts [5]. In spite of this diversity, one may search for possible universal features of collective motion, a context in which the study of "minimal" models is a crucial step. Recently, the investigation of the simplest cases, where the problem is reduced to the competition between a local aligning interaction and some noise, has revealed a wealth of unexpected collective properties. For example, constant speed, self-propelled, *polar* point particles with *ferromagnetic* interactions subjected to noise (as in the Vicsek model [6]) can form a collectively moving fluctuating phase with long-range polar order even in two spatial dimensions [7], with striking properties such as spontaneous segregation into ordered solitary bands moving in a sparse, disordered sea, or anomalous ("giant") density fluctuations [8]. In contrast, active *apolar* particles with *nematic* interactions only exhibit quasi-long-range nematic order in two dimensions with segregation taking the form of a single, strongly-fluctuating, dense structure with longitudinal order and even stronger density fluctuations than in the polar-ferromagnetic case [9, 10, 11].

Noting that these differences reflect those in the local symmetry of particles and their interactions, a third situation can be defined, intermediate between the polar ferromagnetic model and the apolar nematic one, that of self-propelled *polar particles aligning nematically* [12]. Such a mechanism is typically induced by volume exclusion interactions, when elongated particles colliding almost head-on slide past each other, as illustrated schematically in Fig. 1. Thus, self-propelled polar point particles with apolar interactions can be conceived as a minimal model for self-propelled rods interacting by inelastic collisions [13, 14, 15]. Other relevant situations can be found in a biological context, such as gliding myxobacteria moving on a substrate [16], or microtubules driven by molecular motors grafted on a surface [17].

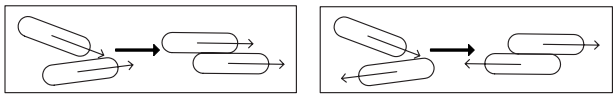

FIG. 1: Nematic alignment of polar particles illustrated by inelastic collisions of rods. Particles incoming at a small angle (left) align "polarly", but those colliding almost head-on slide past each other, maintaining their nematic alignment (right).

In this Letter, we study collections of constant-speed polar point particles interacting locally by nematic alignment in the presence of noise. The simplicity of this model allows us to deal with large numbers of particles, revealing a phenomenology previously unseen in more complicated models sharing the same symmetries [13, 14, 15]. Our study, restricted to two space dimensions, shows in particular collective properties distinctively different from both those of polar-ferromagnetic case and of active nematics: only nematic order arises in spite of the polar nature of the particles, but it seems genuinely long-ranged. Spontaneous density segregation is also observed but it is of a different type and it splits both the (nematically) ordered and the disordered phase in two. In the following, we characterize these four phases and discuss the three transitions separating them.

Our model consists of N point particles moving off-lattice at constant speed v_0. In two dimensions, particle j is defined by its (complex) position $\mathbf{r}_j^t$ and orientation θ_j^t, updated at discrete time steps according to

$$\theta_j^{t+1} = \arg\left[\sum_{k\sim j} \mathrm{sign}\left[\cos(\theta_k^t - \theta_j^t)\right] e^{i\theta_k^t}\right] + \eta\xi_j^t \quad (1)$$

$$\mathbf{r}_j^{t+1} = \mathbf{r}_j^t + v_0\, e^{i\theta_k^{t+1}}\,, \quad (2)$$

where the sum is taken over all particles k within unit distance of j (including j itself), and ξ is a white noise uni-

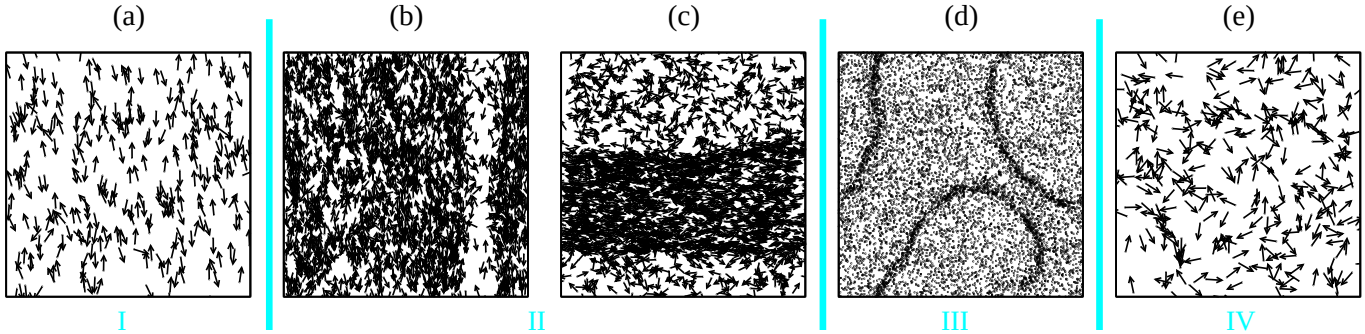

FIG. 2: (color online) (a-c) Typical steady-state snapshots at different noise values (linear size $L = 2048$). (a) $\eta = 0.08$, (b) $\eta = 0.10$, (c) $\eta = 0.13$, (d) $\eta = 0.168$, (e) $\eta = 0.20$. Arrows indicate the polar orientation of particles (except in (d)); only a fraction of the particles are shown for clarity reasons. For a movie corresponding to (d) see [21].

formly distributed in $\left[-\frac{\pi}{2}, \frac{\pi}{2}\right]$ [18]. (A continuous-time version of this model can be found in [19].) The system has two main control parameters: the noise amplitude η, and the particle density $\rho = N/A$, where A is the domain area. We consider periodic boundary conditions. Polar and nematic order can be characterized by means of the two time-dependent global scalar order parameters $P(t) = |\langle \exp(i\theta_j^t)\rangle_j|$ (polar) and $S(t) = |\langle \exp(i2\theta_j^t)\rangle_j|$ (nematic), as well as their asymptotic time averages $P = \langle P(t)\rangle_t$ and $S = \langle S(t)\rangle_t$.

In this work, we focus on the behavior of the system for $\rho = \frac{1}{8}$ and $v_0 = 1/2$, varying η. We start with a brief survey of the stationary states observed in a square domain of linear size $L = 2048$ (Figs. 2-3). Despite the polar nature of the particles, only *nematic* orientational order arises at low noise strengths, while P always remains near zero (not shown). This is in agreement with the findings of [20]. Both the ordered and the disordered regimes are subdivided in two phases, one that is spatially homogeneous (Figs. 2(a,e)), and one where spontaneous density segregation occurs, leading to high-density ordered bands along which the particles move back and forth (Figs. 2(b-d)). A total of four phases is thus observed, labeled I to IV by increasing noise strength hereafter. Phases I and II are nematically ordered, phases III and IV are disordered. Below, we study these four phases more quantitatively.

Phase I, present at the lowest η values, is ordered and spatially homogeneous (Fig. 2a). Its nematic order, which arises quickly from any initial condition, is due to the existence, at any time, of two subpopulations of particles that migrate in opposite directions (Fig. 4a). Statistically of equal size, they constantly exchange particles, those which "turn around". These events occur at exponentially-distributed times τ (Fig. 4b). Increasing system size, the nematic order parameter S is almost constant, decaying *slower than a power law* (Fig. 4c). A good fit of this decay is given by an algebraic approach to a constant asymptotic value S^*. Thus, our data seem to indicate the existence of true long-range nematic order. (Quasi-long-range order, expected classically for two-dimensional nematic phases, is characterized by an algebraic decay of S.) A discussion of this striking fact is given below. Finally, as expected on general grounds for homogeneous ordered phases of active particles [10], phase I exhibits so-called giant number fluctuations: the fluctuations $\Delta n^2 = \langle (n - \langle n\rangle)^2\rangle$ of the average number of particles $\langle n\rangle = \rho\ell^2$ contained in a square of linear size ℓ follow the power law $\Delta n \sim \langle n\rangle^\alpha$ with $\alpha > \frac{1}{2}$ (Fig. 4d). Our estimate of α is compatible to that measured for *polarly* ordered phases $\alpha = 0.8$ [8].

Phase II differs from phase I by the presence, in the steady-state, of a low-density disordered region. In large-enough systems (10^4-10^5 particles for the parameters used here), a narrow, low density channel emerges (Fig. 2b) when increasing η from phase I. It becomes wider at larger η values, so that one can then speak of a high-density ordered band, typically oriented along one of the main axes of the box, amidst a disordered sea (Fig. 2c). Particles travel along the high-density band, turning around or leaving the band from time to time. Within the band, nematic order with properties similar

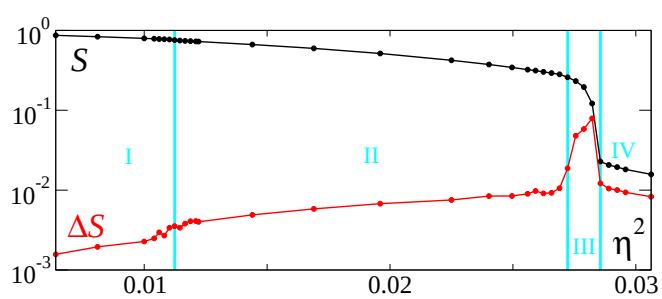

FIG. 3: (color online) Nematic order parameter S (in black) and its rms fluctuations ΔS (in red) as function of the squared noise amplitude η^2 for a square domain of linear size $L = 2048$. Here, and throughout the paper, time-averages are over at least 10^6 timesteps.

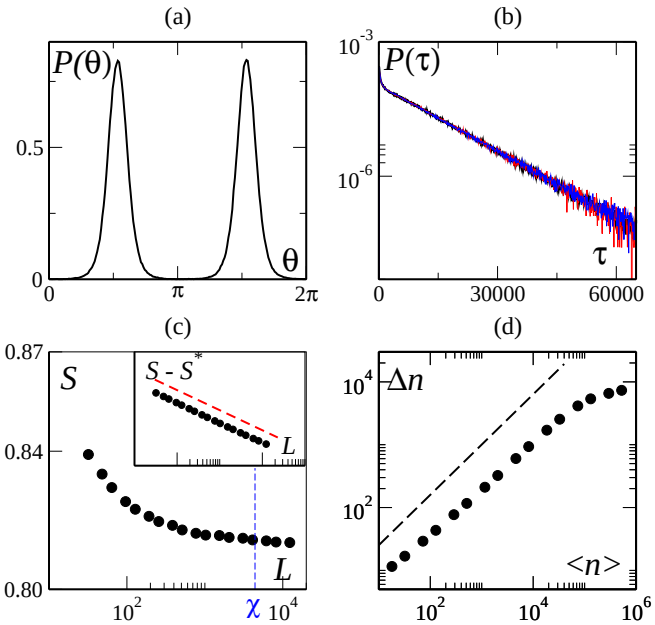

FIG. 4: (color online) Phase I (homogeneous nematic order, $\eta = 0.095$). (a) Polar orientation probability distribution in a system of size $L = 2048$. (b) Distribution of particles transition times τ between the two peaks of (a) for three different system sizes $L = 512$, 1024, and 2048 (black, red, and blue lines respectively). (c) Nematic order parameter S vs system size L in square domains. The vertical red dashed line marks the persistence length $\chi \approx 4400$ (see text). Inset: $S - S^* = 0.813063$ vs L (red dashed line: $L^{-2/3}$ decay). (d) Number fluctuations Δn as a function of average particle number $\langle n \rangle$ (see text) in a system of size $L = 4096$ (dashed line: algebraic growth with exponent 0.8).

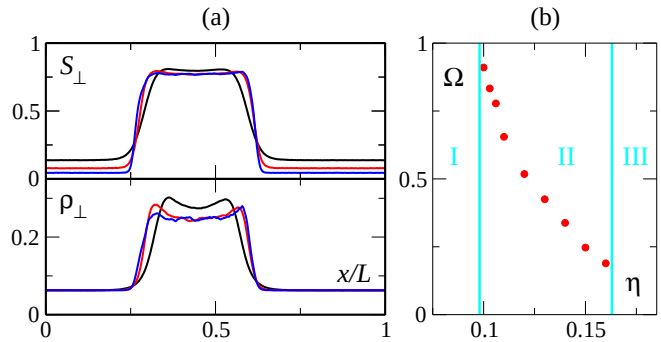

FIG. 5: (color online) Phase II (stable bands) (a) Rescaled transverse profiles in square domains of linear size $L = 512$ (black), 1024 (red), and 2048 (blue) at $\eta = 0.14$. (Data averaged over the longitudinal direction and time, translated to be centered at the same location.) Bottom: density profiles. Top: nematic order parameter profiles. (b) Surface fraction Ω as a function of noise amplitude η (defined here as the width at mid-height of the rescaled S profile).

to those of phase I is found (slow decay of S with system size, giant number fluctuations). The (rescaled) band possesses a well-defined profile with sharper and sharper edges as L increases (Fig. 5a). The fraction area Ω occupied by the band is thus asymptotically independent of system size, and it decreases continuously as the noise strength η increases (Fig. 5b).

In phase III, spontaneous segregation into bands still occurs (for large-enough domains), however these thinner bands are unstable and constantly bend, break, reform, and merge, in an unending spectacular display of space-time chaos (Fig. 2d) [21]. Correspondingly, $S(t)$ fluctuates strongly (Fig. 3) and on very large time scales (Figs. 6a). Nevertheless, these fluctuations behave normally (*i.e.* decrease like $1/\sqrt{N}$, Fig. 6b). Thus, the space-time chaos self-averages, making phase III a bona fide disordered phase, albeit one with huge correlation lengths and times.

Phase IV, observed for the highest noise strengths, exhibits local and global disorder on small length- and time-scales, and is spatially homogeneous (Fig. 2e).

We now discuss briefly the nature of the three transitions that separate the four observed phases (details will appear elsewhere [22]) . The I–II transition, located at $\eta_{\mathrm{I-II}} \simeq 0.098(2)$, is characterized by the emergence of a narrow low-density disordered channel. Within phase II, the emergence of these structures from disordered initial conditions is reminiscent of a nucleation process. Even though the emerging channels might occupy an arbitrarily small proportion of space near the transition ($\Omega \sim 1$ for $\eta \gtrsim \eta_{\mathrm{I-II}}$), they seem to possess a minimum absolute width. These facts suggest a discontinuous I–II transition. The transition between phase II and III, located near $\eta_{\mathrm{II-III}} \simeq 0.163(1)$, constitutes the order-disorder transition of the model. As mentioned above, it resembles a long-but-finite wavelength instability of the band (see, e.g., Fig. 6c) and does not appear as a fluctuation-driven phase transition. The disorder-disorder transition between phases III and IV occurs near $\eta_{\mathrm{III-IV}} \simeq 0.169(1)$, where the instantaneous order parameter $S(t)$ exhibits a bistable behavior between a low value, fast fluctuating state typical of phase IV and a larger amplitude, slowly fluctuating one characteristic of phase III. This bistability, leading to a bimodal order parameter distribution, suggests a discontinuous phase transition.

At this point, the most crucial question is perhaps that of the stability of the nematic order observed in phases I and II. Indeed, much of what we described above for large but finite systems relies on our conclusion of possible truly long-range (asymptotic) order (Fig. 4c). On the one hand, one could argue that the exponential distributions of flight times between the two opposite polar orientations (Fig. 4b) define a finite persistence time τ and a corresponding finite persistence lengthscale $\chi \approx v_0\tau$ (indicated by the blue dashed line in Fig. 4c). Therefore, at scales much larger than χ, the polar nature of our particles could become irrelevant, and the system would then

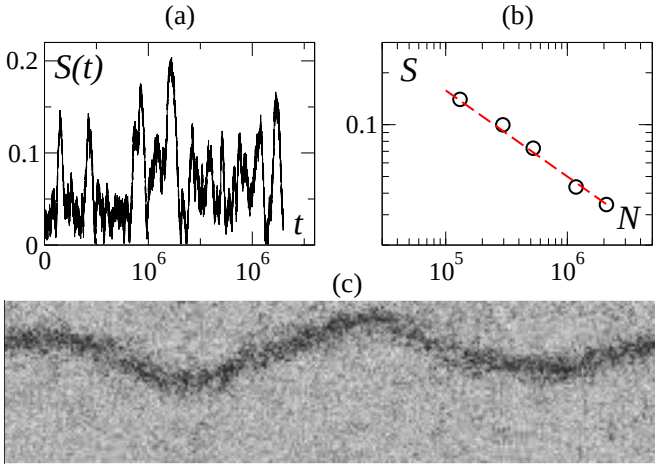

FIG. 6: Phase III (unstable bands, $\eta = 0168$). (a) Typical nematic order parameter time series for a system of linear size $L = 2048$. (b) S vs N in square domains of increasing sizes. (The dashed line marks a $1/\sqrt{N}$ decay.) (c) Snapshot of coarse-grained density field during the growth of the instability of an initially straight band in a 2048×512 domain.

behave like a fully nematic one, with only quasi-long-range order. As of now, we have been able to probe systems sizes up to three or four times the persistence length χ. So far, as shown in Fig. 4c, these systems comprising up to twenty million particles show no sign of breakdown of order. On the other hand, χ is a single-particle quantity. Even though it is finite and system size independent, particles travel in rather dense *polar* packets which have flights longer than χ. Indeed, the giant density fluctuations reported (Fig. 4d) indicate that denser, more ordered, and hence probably longer-lived packets occur in larger systems. Unfortunately, packets' flight times are hard to define and measure [22]. But should this "polar packet lifetime" diverge with system size, then one would have a mechanism opening the door for the emergence of true long-range nematic order. To summarize this discussion, nematic order could break down for sizes much larger than χ, but our data (Figs. 4c,d) and the argument above suggest the picture of two opposite polar components each with true long-range order (as in fully-polar models [23]) summing up to true nematic order.

Further work is thus needed, but most of our results are rather robust. For instance, the introduction of some soft-core short-range repulsion between particles does *not* modify our main findings [22]. Thus, these are not due to the pointwise nature of the particles, and should also be observed in previous, more detailed models of self-propelled rods if sufficiently-large populations are considered. We note also that our results, and in particular the instability and space-time chaotic motion of the spontaneously segregated bands (phases II and III) [21], are reminiscent of the streaming and swirling regime which characterizes the aggregation of myxobacteria [16, 24] and thus our model could prove relevant in this context.

At a more general level, our findings reveal unexpected emergent behavior among even the simplest situations giving rise to collective motion. Our model of self-propelled polar objects aligning nematically stands out as a member of a universality class distinct from both that of the Vicsek model [6, 7, 8] and of active nematics [9]. Thus, in this out-of-equilibrium context, the symmetries of the moving particles and of their interactions must be considered separately and are both relevant ingredients.

We thank J. Toner and S. Ramaswamy for fruitful discussions. This work was partially funded by the French ANR projects "Morphoscale" and "Panurge", and the German DFG grants DE842/2, SFB 555, and GRK 1558.

[1] *Three Dimensional Animals Groups*, edited by J.K. Parrish and W.M Hamner (Cambridge University Press, Cambridge, England, 1997), and references therein.
[2] D. Helbing, I. Farkas, and T. Vicsek, Nature (London) **407**, 487 (2000).
[3] A. Sokolov, *et al.*, Phys. Rev. Lett. **98**, 158102 (2007).
[4] E. Ben-Jacob et al., Adv. Phys. **49**, 395 (2000).
[5] P. Romanczuk, I.D. Couzin, and L. Schimansky-Geier, Phys. Rev. Lett. **102**, 010602 (2009).
[6] T. Vicsek *et al.*, Phys. Rev. Lett. **75**, 1226 (1995).
[7] J. Toner, and Y. Tu, Phys. Rev. Lett. **75**, 4326 (1995); Phys. Rev. E **58**, 4828 (1998).
[8] H. Chaté, *et al.*, Phys. Rev. E **77**, 046113 (2008); G. Grégoire and H. Chaté, Phys. Rev. Lett. **92**, 025702 (2004).
[9] H. Chaté, F. Ginelli, and R. Montagne, Phys. Rev. Lett. **96**, 180602 (2006).
[10] S. Ramaswamy, R.A. Simha, and J. Toner, Europhys. Lett. **62**, 196 (2003).
[11] S. Mishra and S. Ramaswamy, Phys. Rev. Lett. **97**, 090602 (2006).
[12] The reverse case of active nematic particles with a ferromagnetic interaction does not make sense.
[13] F. Peruani, A. Deutsch, and M. Bär, Phys. Rev. E **74**, 030904(R) (2006).
[14] A. Kudrolli *et al.*, Phys. Rev. Lett. **100**, 058001 (2008).
[15] H.H. Wensink and H. Löwen, Phys. Rev. E **78**, 031409 (2008).
[16] L. Jelsbak and L. Sogaard-Andersen, Proc. Natl. Acad. Sci. USA **99**, 2032 (2002); D. Kaiser, Nat. Rev. Microbiol. **1**, 45 (2003).
[17] F. Ziebert *et al.*, Eur. Phys. J. E **28**, 401 (2009).
[18] Note that the sign operation in Eq. (1) makes it invariant under the rotation $\theta_k^t \to \theta_k^t + \pi$ of any of the neighboring particles, *i.e.* the interaction is nematically symmetric.
[19] F. Peruani, A. Deutsch, and M. Bär, Eur. Phys. J-Spec. Top.,**157**, 111 (2008).
[20] A. Baskaran and M.C. Marchetti, Phys. Rev. E **77**, 011920 (2008); Phys. Rev. Lett. **101**, 268101 (2008).
[21] See EPAPS Document No. XXX for a movie.
[22] F. Peruani, F. Ginelli, and H. Chaté, to be published.
[23] This is also suggested by our observation that the density

fluctuations are governed by the same exponent as in the polar case (Fig. 4d).

[24] D.R. Zusman, *et al.*, Nature (London) **5**, 862 (2007), and references therein.